Proceedings of the ASME 2010 3rd Joint US-European Fluids Engineering Summer Meeting and 8th International Conference on Nanochannels, Microchannels, and Minichannels
FEDSM-ICNMM2010
August 1-5, 2010, Montreal, Canada

FEDSM-ICNMM2010-31118

FLOW SIMULATION AND DIAGANOSIS THROUGH HYDRAULIC TURBINES USING A RNG k-ω TUR BULENCE MODEL

Shuhong LIU
Tel (Fax): +86-10-62794735, E-mail: liushuhong@mail.tsinghua.edu.cn
State Key Laboratory of Hydro science & Hydraulic Eng. Dept.of Thermal Eng., Tsinghua University, Beijing 100084, China

Xiaojing WU,
State Key Laboratory for Turbulence and Complex Sysytem, College of Eng.,
Peking University, Beijing 100871, China

Yulin WU
State Key Laboratory of Hydro science & Hydraulic Eng., Dept. of Thermal Eng.,
Tsinghua University, Beijing 100084, China

ABSTRACT

Francis turbine is widely employed in large scale hydro-power stations in the world with main characteristics of efficiency, stability and cavitation. In practical establishment, each large power station must develop a new Francis turbine for its special natural condition and requirement, such as higher efficiency for utilization of natural resources. CFD has been developed greatly and helped a lot in hydraulic design stage of the turbine.

In this paper, firstly, a new RNG $k-\omega$ turbulence model is proposed based on the RNG $k-\varepsilon$ model, which brings the nonlinear term of the mean fluid flow transition to the ω equation in the original $k-\omega$ model. And, this RNG $k-\omega$ model has been used to predict the energy performances for Francis turbine. Then, the flow diagnosis method in the turbine runner based on vorticity parameters is presented, following the detailed flow behavior revealed. Finally, the simulation results for different model Francis turbines have been compared and analyzed for optimizing the energy performances of the turbine. The model test results indicate that the efficiency of hydraulic turbine has been improved from 93.6% to 94.5%.

Key words: flow simulation, flow diagnosis, RNG $k-\omega$ turbulence model, Francis turbine

INTRODUCTION

During the last few years, dynamic analysis of hydraulic turbines has become a major issue. Customers request more efficient and, at the same time, less expensive turbines. With the increasing capacity and size of hydraulic turbines, vibration of the turbine component structure and the rotating system severely influences the operation of turbines and the safety of power house where turbines are installed. All the demands need the technique of computational fluid dynamics (CFD) to be used in hydraulic design stage of the turbine. CFD has been developed greatly. Some scholars have focused on new methods, for example, the lattice Boltzmann method [1], and the large eddy simulation [2]. But in most industrial flows include turbulent flows, CFD methods solve Reynolds-averaged Navier-Stokes (RANS) equations mainly, using turbulence models to compute the averaged turbulent stresses, for example, to compute the unsteady flows [3] and even the cavitating flows [4] in hydraulic turbines.

In this paper, a RNG $k-\omega$ turbulence model is proposed based on the RNG $k-\varepsilon$ model [5, 6], which brings the nonlinear term of the mean fluid flow transition to the ω equation in the original $k-\omega$ model of Wilcox [7]. The RNG $k-\omega$ model has been used to predict the energy performances for Francis turbine. Then, the flow diagnosis method in the turbine runner based on vorticity parameters [8] is presented. Vorticity parameters can be used to reveal the detailed flow behavior better than ordinary flow parameters, such as velocity and pressure [9]. The simulation results for different model Francis turbines have been compared and analyzed, in order to optimize the energy performances of the turbine.

TURBULENCE MODEL AND SIMULATION METHODS

RNG k-ω t urbulence model

Based on the RNG $k-\varepsilon$ model [5, 6] and the expression of the definition of the turbulent dissipation frequency, ω, its equation, which has the nonlinear term of the mean fluid flow transition, R_ω, is as follows

$$\rho\frac{\mathrm{D}\omega}{\mathrm{D}t}=P_\omega-\Phi_\omega+D_\omega-R_\omega \tag{1}$$

where

$$P_\omega = \left(\frac{1}{C_k k} C_{1\varepsilon} \frac{\varepsilon}{k} - \frac{\omega}{k}\right) G_k = (C_{1\varepsilon} - 1)\frac{\omega}{k} G_k \tag{2-1}$$

$$\Phi_\omega = \frac{1}{C_k k} C_{2\varepsilon} \frac{\varepsilon^2}{k} - \frac{\omega}{k} C_k \omega k = (C_{2\varepsilon} - 1) C_k \omega^2 \tag{2-2}$$

$$\begin{aligned} D_\omega &= \frac{1}{C_k k}\frac{\partial}{\partial x_j}\left(\frac{\mu_t}{\sigma_\varepsilon}\frac{\partial \varepsilon}{\partial x_j}\right) - \frac{\omega}{k}\frac{\partial}{\partial x_j}\left(\frac{\mu_t}{\sigma_k}\frac{\partial k}{\partial x_j}\right) \\ &= \frac{\mu_t}{k}\left(\frac{1}{\sigma_\varepsilon} + \frac{1}{\sigma_k}\right)\frac{\partial k}{\partial x_j}\frac{\partial \omega}{\partial x_j} + \mu_t \frac{\omega}{k}\left(\frac{1}{\sigma_\varepsilon} - \frac{1}{\sigma_k}\right)\frac{\partial^2 k}{\partial x_j^2} \\ &+ \mu_t \frac{\omega}{k^2}\left(\frac{1}{\sigma_\varepsilon} - \frac{1}{\sigma_k}\right)\left(\frac{\partial k}{\partial x_j}\right)^2 + \frac{\partial}{\partial x_j}\left(\frac{\mu_t}{\sigma_\varepsilon}\frac{\partial \omega}{\partial x_j}\right) \end{aligned} \tag{2-3}$$

$$R_\omega = \frac{1}{C_k k}\frac{C_\mu \rho \eta^3 (1 - \eta/\eta_0)}{1 + \beta \eta^3}\frac{\varepsilon^2}{k} = \frac{C_\mu C_k \rho \eta^3 (1 - \eta/\eta_0)}{1 + \beta \eta^3}\omega^2 \tag{2-4}$$

Equation (1) and Eqs. (2-1) to (2-4) are the model transport equations for the turbulent dissipation rate frequency ω according to the RNG theory and form a RNG $k-\omega$ turbulence model, if combined with the corresponding turbulent kinetic energy equation in the form [7]:

$$\rho \frac{\mathrm{D}k}{\mathrm{D}t} = \frac{\partial}{\partial x_j}\left(\left(\mu + \frac{\mu_t}{\sigma_k}\right)\frac{\partial k}{\partial x_j}\right) + G_k - \rho C_k k \omega \tag{3}$$

Turbulent viscosity is modeled as:

$$\mu_t = C_\mu \rho \frac{k}{\omega} \tag{4}$$

where $C_\mu = 0.0845$, $C_{1\varepsilon} = 1.42$, $C_{2\varepsilon} = 1.68$, $C_k = 0.8$, $C_\varepsilon = 0.8$ (C_k and C_ε can be chosen as 0.7194 as theoretical), $\eta_0 = 4.38$, $\beta = 0.012$ and $\eta \equiv \frac{S}{C_k \omega}$, $G_k = \mu_t S^2$, $S \equiv \sqrt{2 S_{ij} S_{ij}}$, $S_{ij} = \frac{1}{2}\left(\frac{\partial u_i}{\partial x_j} + \frac{\partial u_j}{\partial x_i}\right)$.

3D turbulent flow simulation domain

The 3D steady turbulent simulation has been conducted, which enables the prediction of hydraulic turbine performances [4]. In hydraulic turbine, the present computational domain covers the complete flow passage starting from the inlet of spiral casing through out stay vanes, guide vanes, runner to the outlet of draft tube, including the rotor-stator interactions by frozen mesh between the stationary guide vanes and the rotating runner and between the runner and the draft tube [3, 4].

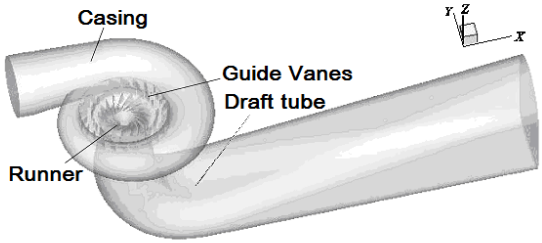

Fig. 1 Computational domain

Boundary conditions

The boundary conditions for steady flow computation are as follows. On the inlet of the calculated domain, the static pressure is given by the test head with velocity normal to inlet boundary. The inlet velocity is determined by the given flow rate.

On the outlet of the calculated domain, to satisfy the flow continuity condition, correction to the outlet velocity distribution should be made to off-set the flow rate difference between the inlet and the outlet during the calculation process.

It is assumed that in the normal direction of boundaries except for the inlet boundary, gradients of pressure, k and ω are zero. The wall function is employed for the vicinity of the fixed wall, and the non-slip boundary condition is applied too. For rotating boundary of runner, the boundary is moving at a velocity equal to tangent velocity of the runner periphery.

Numerical simulation treatment

A mesh with 2,000,000 elements was finally employed for the whole flow passage after the mesh independence study. After test run, this mesh was fine enough to satisfy $y^+ < 40$ near the wall and to obtain required features of friction and pressure [4].

The soft ware CFX is used to make the numerical simulation. In the simulation, the second order upwind scheme is used for discretization of convective term and the second order central scheme for discretization of diffusion term and other source terms. The direct coupling method is used to solve the incompressible flow in the present simulation. The discrete momentum equations and the continuity equation for the complete flow field are solved together without iteration and corrections. This numerical method will need large computer storage, but it will improve the stability in the numerical procedure [4].

FLOW DIAGNOSIS

A new approach to aerodynamic diagnostics and inverse design based on the theory of boundary vorticity dynamics has been presented and illustrated by various numerical examples [10]. By integrating the stresses over the wall surface S, the force $\boldsymbol{F}$ and momentum $\boldsymbol{M}$ acting on the body surfaces,

$\sum$, due to the fluid flow can be derived to give the following forms [8]:

$$\boldsymbol{F} = \int_{\sum} \mu_{\text{eff}} (\boldsymbol{n} \times \boldsymbol{\omega}) \mathrm{d}S - \frac{\mu}{D} \int_{\sum} \boldsymbol{r} \times \left[\boldsymbol{n} \times (\nabla \times \mu_{\text{eff}} \boldsymbol{\omega}) \right] \mathrm{d}S \qquad (4)$$

$$\boldsymbol{M} = \int_{\sum} \mu_{\text{eff}} \boldsymbol{r} \times (\boldsymbol{n} \times \boldsymbol{\omega}) \mathrm{d}S + \frac{1}{2} \int_{\sum} r^2 \boldsymbol{n} \times (\nabla \times \mu_{\text{eff}} \boldsymbol{\omega}) \mathrm{d}S \qquad (5)$$

where μ_{eff} is the effective viscosity including the eddy viscosity and molecular one; $\boldsymbol{n}$ the unit normal vector perpendicular to body surfaces; $\boldsymbol{\omega}$ the vorticity vector on fluid flow field and $\boldsymbol{r}$ is radium vector. The integral functions in Eqs. (4) and (5) are the variables of flow diagnosis on the surfaces as

$$\boldsymbol{L}_1 = \mu_{\text{eff}} (\boldsymbol{n} \times \boldsymbol{\omega}) \qquad \boldsymbol{L}_2 = \mu_{\text{eff}} \boldsymbol{r} \times (\boldsymbol{n} \times (\nabla \times \boldsymbol{\omega})) \qquad (6)$$

$$\boldsymbol{L}_3 = \mu_{\text{eff}} \boldsymbol{r} \times (\boldsymbol{n} \times \boldsymbol{\omega}) \qquad \boldsymbol{L}_4 = \mu_{\text{eff}} r^2 \boldsymbol{n} \times (\nabla \times \boldsymbol{\omega}) \qquad (7)$$

where $\boldsymbol{L}_3$ is called as the vorticity moment and $\boldsymbol{L}_4$ the vorticity moment graduate.

RESULTS AND DISCUSSIONS

The turbulent flow in the original model Francis turbine and its performance test has been carried out. The efficiency at the optimum operation case (guide vane opening is 18 mm) is about 93.5%. This value is not satisfied with the power station requirement. The optimizing design has been required to increase the efficiency of the model turbine. According to results of the 3D turbulent flow simulation, the variables of flow diagnosis on the runner blade surfaces, $\boldsymbol{L}_1$ to $\boldsymbol{L}_4$, could be obtained, then the new design of the runner blade should be made based on the distribution of $\boldsymbol{L}_1$ to $\boldsymbol{L}_4$. The iterative design has been repeated several times. The final results of the runner geometries are satisfied as shown in Fig. 2 and Fig. 3.

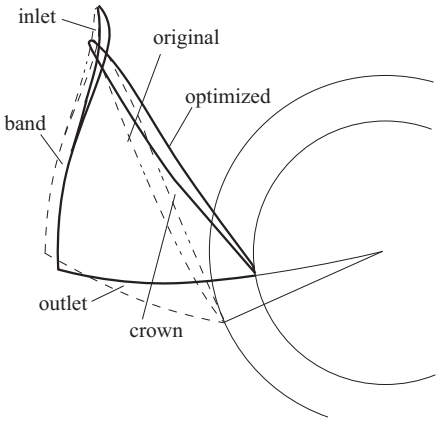

Fig. 2 Planform of original and optimized runners

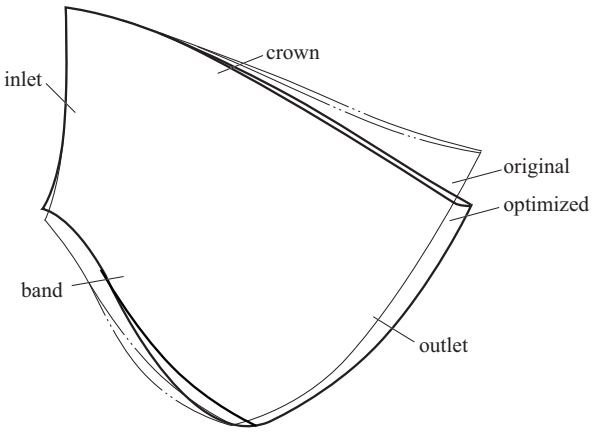

Fig. 3 Side elevation of original

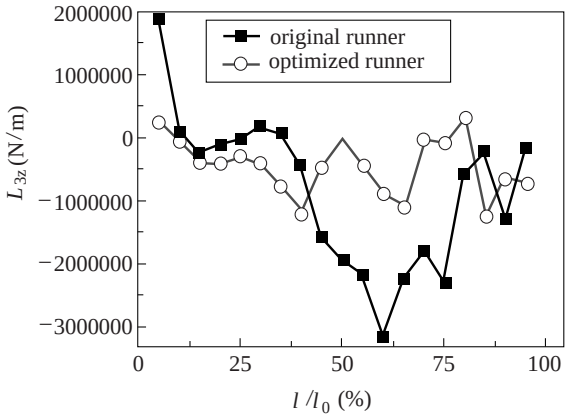

(a) Pressure side of runner blade

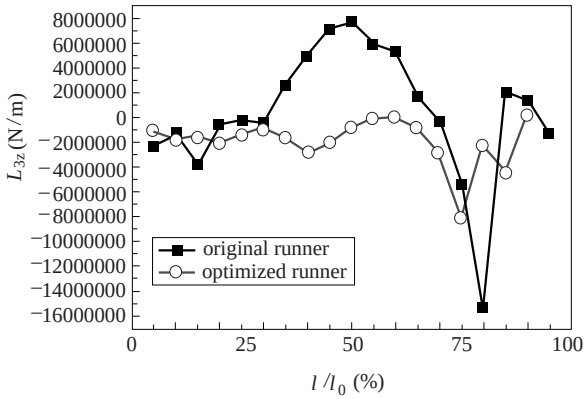

(b) Suction side of runner blade

Fig. 4 L_{3z} distributions of runner blade (Optimum case, G.V. opening: 18mm)

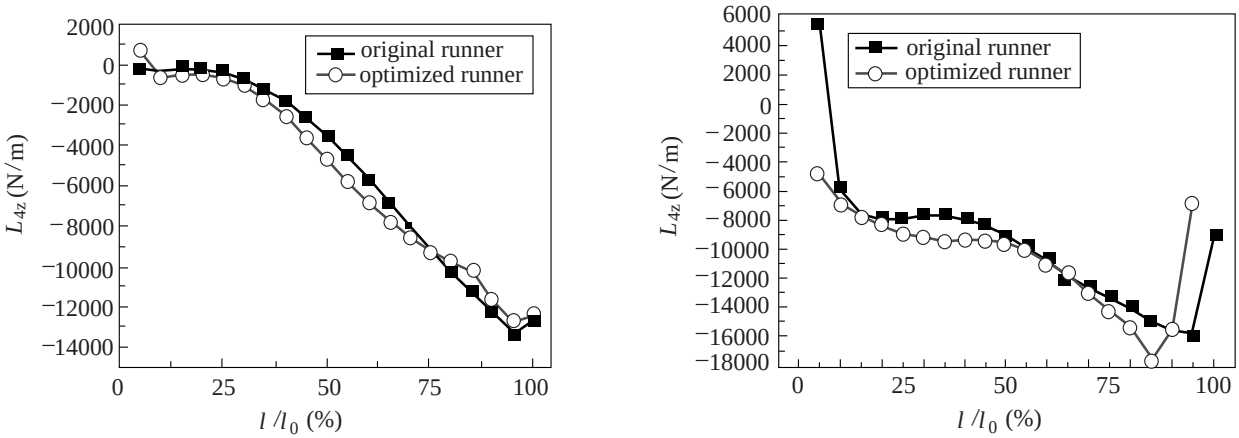

(a) Suction side of runner blade (b) Pressure side of runner blade

Fig. 5 L_{4z} distributions of runner blade (Optimum case, G.V. opening: 18mm)

Table 1 Parameters comparison of test data and calculated results (Improved runner)

Guide vane opening	Turbulence model	Flow rate (kg/s)	Head (m)	Torque on runner (N m)		Hydro efficiency (%)	
				Cal.	Test	Cal.	Test.
	RNG $k-\varepsilon$		20.1	648.0		92.6	
14 mm	$k-\omega$	264.7	20.0	623.5	675.0	91.5	93.0
	RNG $k-\omega$		19.9	680.2		93.5	
	RNG $k-\varepsilon$		20.0	820.2		93.3	
18 mm	$k-\omega$	329.6	20.2	790.3	855.0	92.5	94.4
	RNG $k-\omega$		19.8	863.4		94.7	
	RNG $k-\varepsilon$		20.1	930.8		93.0	
20 mm	$k-\omega$	370.3	19.9	890.5	950.3	92.1	94.2
	RNG $k-\omega$		20.0	950.6		94.4	
	RNG $k-\varepsilon$		20.0	1037.2		91.2	
23 mm	$k-\omega$	430.9	20.1	1000.1	1075.0	89.7	91.8
	RNG $k-\omega$		20.0	1086.0		91.9	

The averaged L_{3z} and L_{4z} distributions of original and optimized runner blade are shown in Figs. 4 and 5 at optimum case of guide vane opening 18 mm of hydraulic turbine. L_{3z} and L_{4z} are the projections of vectors, $\boldsymbol{L}_3$ and $\boldsymbol{L}_4$, on the ordinate z which is the rotation axis of the turbine runner. L_{3z} is the reflection of pressure distribution on blade surfaces; and L_{4z} of friction share distribution. l is the length from the leading edge of runner, and l_0 is from the leading edge to the trailing edge of runner. They are located in the middle from crown to band of runner.

The distribution comparison between the original runner and the optimum one indicats that the original L_{3z} changes from large positive value to negative value on the most of pressure side, and the optimum L_{3z} keeps a near constant value. That means the vorticity of improved runner is not changed largely and the great variation of vortex does not occur.

For both runners, L_{4z} changes steadily from the leading edge to trailing edge on the pressure side. The difference of L_{4z} between the original runner and improved one is not large. Compared with the improved one, at the leading edge, the L_{4z} on the suction side of the original runner blade drops greatly. This indicates that the improved runner can obtain more moment of friction force on the runner blade, resulting from the increasing of water thrust along the tangential direction.

To verify the accuracy of calculation and the optimization of hydraulic design, calculated results of performances of the optimized turbine with the RNG $k-\omega$ turbulence model are compared with experiment data and with calculated results of other two turbulent models, shown in Table 1.

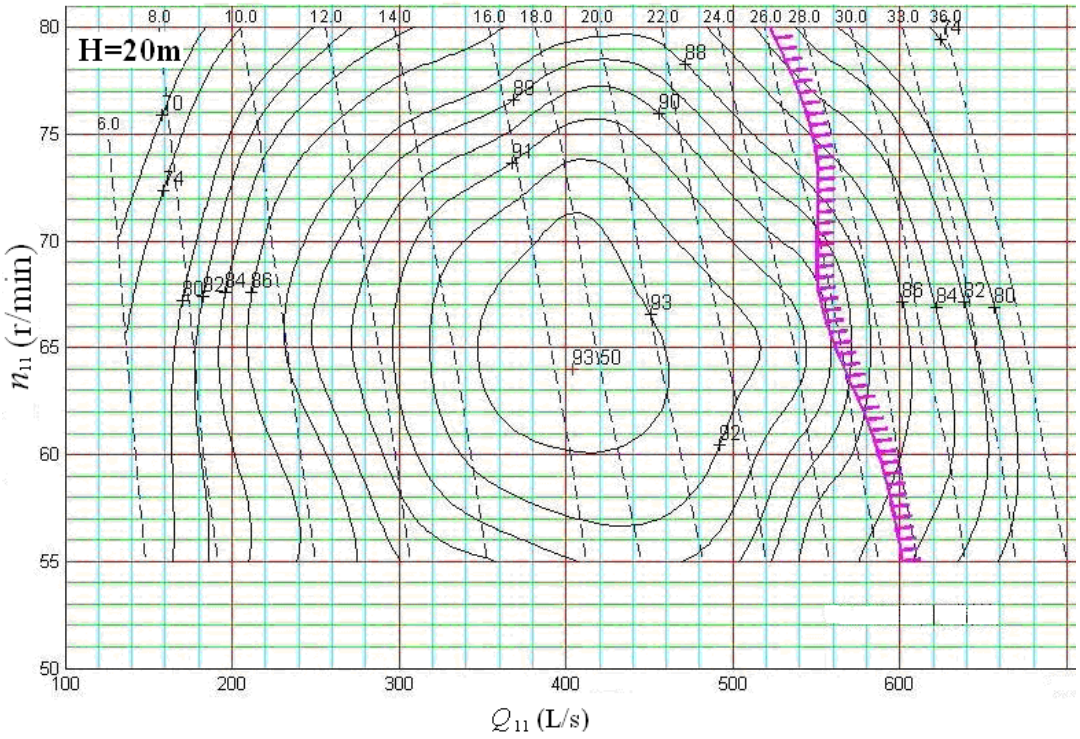

(a) Original runner

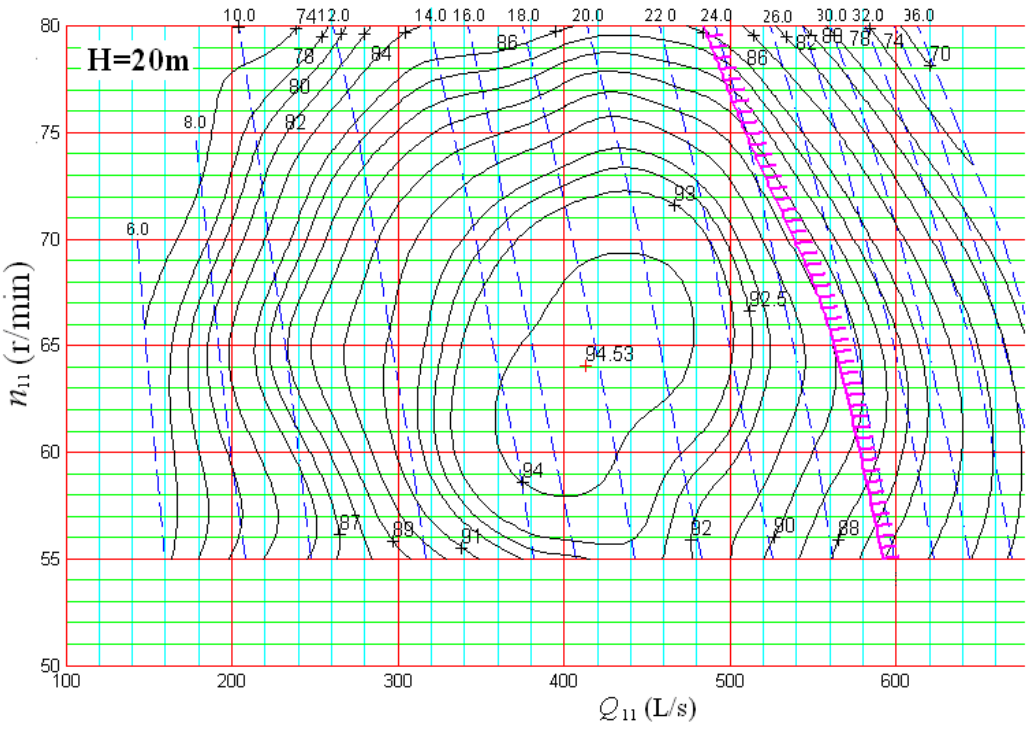

(b) Improved runner

Fig. 6 Model Hill-chart of two runners

In this calculation, the inlet velocity distribution is given as the boundary condition, after the calculation, one can get the total pressure difference between the inlet of spiral casing and the out let of draft tube, which is the working head upon the turbine. The work head results are around 20m with a little error. Results in Table 1 indicate that, all models could predict the working head accurately. Other energy performances are the water moment acting on runner and the hydraulic efficiency. The calculations with different turbulence models could predict the efficiency with good agreement to the test data, which are able to be used in engineering. Among them, the RNG $k-\omega$ model has better data than those by other two models.

Besides, the predicted efficiency by the RNG $k-\omega$ model is little higher than the test data, while other model results are lower than the test results. Because in the experiment, besides the hydraulic loss, the volumetric and mechanical losses still exist even they have been decreased to vary small amount by nowadays high technology. Therefore, the present RNG $k-\omega$ model can provide reasonable results, which is because the additional nonlinear term in the dissipation rate frequency equation predicts the dissipation rate with small value.

Figure 6 shows the tested model hill-chats with both the original runner and improved runner. Comparing their hill-charts, similar distributions are observed. Both runners provide very similar parameters under the condition with maximum efficiency, unit flow rate of 420l/s and unit rotational speed of 65rpm. The both flow rates under limited conditions are in the range of 550-560l/s, with satisfied the required power output. However, the hydraulic efficiencies are a little bit different. The highest for the original and improved runners are 93.6% and 94.5%; while efficiencies under limited conditions are 88% and 90.5%. Their differences are about 1% and 2% respectively. As a conclusion, the performance of improved runner is better than that of the original one.

CONCLUDING REMARKS

The vorticity moment and the vorticity moment graduate can be used for flow diagnosis in hydraulic turbine runner to improve its efficiency.

The 3D steady turbulent flow simulation, developed in this paper with the new RNG $k-\omega$ model, is used to predict its energy performances of Francis turbine. The predicted results are more reasonable and closer to tests data than the results from the RNG $k-\varepsilon$ model and original $k-\omega$ model.

ACKNOWLEDGMENTS

The research work was funded by Chinese National Foundation of Natural Science (No. 10532010) and by the National Key Technology R&D Program in China. Authors also would like to express their thanks to the support by the Project 2010-ZY-5.

REFERENCES

[1] Yang. F. et al. Numerical study on tranverse-axis rotary viscous pump and hydropulser mechanism, Int. J. Nonlin. Sci. Num., 7(2006): 263-268.

[2] Tang, X.L.et al. Numerical models for turbulent flows through a centrifugal impeller, Int. J. Nonlin. Sci. Num., 9(2008): 81-88.

[3] Liu, S.H. et al. Pressure fluctuation prediction of a model Kaplan turbine by unsteady turbulent flow simulation, Journal of Fluids Eng., 131(2009): 101102.

[4] Liu, S.H. et al. Cavitating turbulent flow simulation in a Francis turbine based on mixture model, Journal of Fluids Eng.,.131(2009): 051302.

[5] Yakhot, V. et al. Development of turbulence models for shear flows by a double expansion technique. Physics of Fluids A, 4(1992):1510-1520.

[6] Smith, L.M and Woodruff, S.L. Renormalization-group analysis of turbulence. Annual Review of Fluid Mechanics,.30 (1998): 275-310.

[7] Wilcox, D.C. Re-assessment of the scale-determining equation for advanced turbulence models. AIAA Journal, 26 (1988):1414-1421.

[8] Liu, S.H. et al. Vorticity analysis of a cavitating two-phase flow in rotating, Int. J. Nonlin. Sci. Num., 10(2009): 599-613.

[9] Zhang R.K. et al. The physical origin of severe low-frequency pressure fluctuations in giant Francis turbines, Mod. Phys. Lett. B, 19(2005): 1527-1530.

[10] Wu, J.Z. et al. A vorticity dynamics theory of three dimensional flow separation. Phys. Fluids, 12(2000): 1932-1954.